



# Journal of Applied Sciences

ISSN 1812-5654

**science**  
alert

**ANSI***net*  
an open access publisher  
<http://ansinet.com>

## Characterization of the Size Distribution of Mountains Extracted from Multiscale Digital Elevation Models

<sup>1</sup>S. Dinesh and <sup>2</sup>M.H. Ahmad Fadzil

<sup>1</sup>Science and Technology Research Institute for Defence (STRIDE), Ministry of Defence, Malaysia

<sup>2</sup>Faculty of Electrical and Electronics Engineering, University Teknologi Petronas

---

**Abstract:** In general, analysis of mountains is performed at singular scales of measurement. However, analysis of a location at multiple scales allows for a greater amount of information to be extracted from a DEM about the spatial characteristics of a feature. In this study, the variation in the spatial extent over which mountains are defined is used as the basis to characterize the size distribution of mountains. First, the lifting scheme is used to generate multiscale DEMs. Mountains extraction is then performed on the generated multiscale DEMs. The size distribution of the extracted mountains is characterized by implementing opening by reconstruction iteratively on the extracted mountains using square kernels of increasing size. A power law relationship is observed between the number and total area of mountain objects remaining. This power law arises as a consequence of the fractal properties of the size distribution of mountains extracted from multiscale DEMs.

**Key words:** Multiscale digital elevation models, lifting scheme, size distribution, opening by reconstruction, power law, fractal dimension

---

### INTRODUCTION

Mountains are the portions a terrain that are sufficiently elevated above the surrounding land (greater than 300 to 600 m) and have comparatively steep sides. In a mountain, two parts are distinctive:

- The summit, the highest point (the peak) or the highest ridges
- The mountainside, the part of a mountain between the summit and the foot (Bates and Jackson, 1987).

The mapping of mountains is generally performed manually through fieldwork and visual interpretation of topographic maps, which is a time consuming and labor intensive activity. In recent times, extraction techniques have evolved from manual through computer assisted to automated methods; with Digital Elevation Models (DEMs) as the input data. In seeking the efficient extraction of mountains from DEMs, various algorithms have been proposed (Graff and Usery, 1993; Miliareisis and Argialas, 1999; Miliareisis, 2000; Dinesh, 2006). Dinesh (2006) proposes a mathematical morphological based mountain extraction algorithm. First, ultimate erosion is performed on the DEM to extract the peaks. Conditional dilation is performed on the extracted peaks to obtain the mountains of the DEM.

Feature detection and characterization often need to be performed at different of scales measurement. Wood (1996a, b) shows that analysis of a location at multiple scales allows for a greater amount of information to be extracted from a DEM about the spatial characteristics of a feature. The term scale refers to combination of both spatial extent and spatial detail or resolution (Tate and Wood, 2001). In this study, the variation in the spatial extent over which mountains are defined is used as the basis to characterize the size distribution of mountains. It is shown, via power law relationships, that the size distribution of mountains possesses fractal properties.

### MATHEMATICAL MORPHOLOGY

Mathematical morphology is a branch of image processing that deals with the extraction of image components that are useful for representational and descriptive purposes. Mathematical morphology is well suited to the processing of elevation data because in morphology, any image is viewed as a topographic surface, the grey level of a pixel standing for its elevation (Soille and Ansoult, 1990). The fundamental morphological operators are discussed in Matheron (1975), Serra (1982) and Soille (2003). Morphological operators generally require two inputs; the input image A,

which can be in binary or grayscale form and the kernel B, which is used to determine the precise effect of the operator.

Dilation sets the pixel values within the kernel to the maximum value of the pixel neighbourhood. The dilation operation is expressed as:

$$A \oplus B = \{a+b: a \in A, b \in B\} \quad (1)$$

Erosion sets the pixels values within the kernel to the minimum value of the kernel. Erosion is the dual operator of dilation:

$$A \ominus B \subset (A^\circ \oplus B)^\circ \quad (2)$$

An opening (Eq. 3) is defined as an erosion followed by a dilation using the same kernel for both operation. Binary opening preserves foreground regions that have a similar shape to this kernel, or that can completely contain the kernel, while eliminating all other regions of foreground pixels.

$$A^\circ B = (A \ominus B) \oplus B \quad (3)$$

Morphological reconstruction allows for the isolation of certain features within an image based on the manipulation of a mask image X and a marker image Y. It is founded on the concept of geodesic transformations, where dilations or erosion of a marker image are performed until stability is achieved (represented by a mask image) (Vincent, 1993).

The geodesic dilation,  $\delta^g$  used in the reconstruction process is performed through iteration of elementary geodesic dilations,  $\delta_{(1)}$ , until stability is achieved.

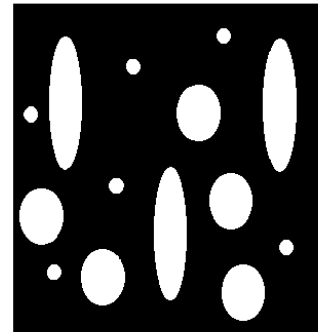
$$\delta^g(Y) = \delta_{(1)}(Y) \circ \delta_{(1)}(Y) \circ \delta_{(1)}(Y) \dots \text{until stability} \quad (4)$$

The elementary dilation process is performed using a standard dilation of size one followed by an intersection.

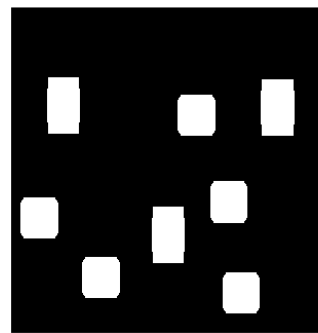
$$\delta_{(1)}(Y) = Y \oplus B \cap X \quad (5)$$

The operation in Eq. 6 is used for elementary dilation in binary reconstruction. In grayscale reconstruction, the intersection in the equation is replaced with a pointwise minimum (Vincent, 1993).

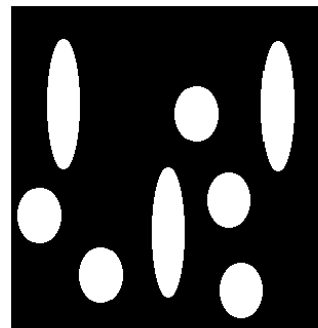
Morphological reconstruction is a useful filtering tool. Figure 1a shows an image with circles of various sizes. In order to filter the smaller sized circles, first opening is performed using a square kernel of size 30. The circles that are unable to completely contain the kernel are



(a)



(b)



(c)

Fig. 1: The application of morphological reconstruction in filtering: (a) The original image, (b) The opened image and (c) The reconstructed image

removed, while the shape of remaining circles is altered (Fig. 1b). Morphological reconstruction is implemented with Fig. 1a being the mask and Fig. 1b being the marker. This restores the original shape of the remaining circles (Fig. 1c). This process is known as opening by reconstruction.

#### GENERATION OF MULTISCALE DEMs USING THE LIFTING SCHEME

In this study, multiscaling is performed using the lifting scheme (Sweldens, 1996, 1997). The lifting scheme

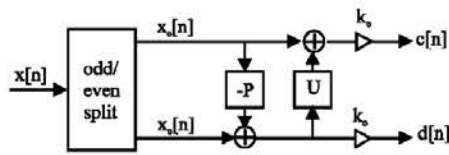


Fig. 2: Lifting stage: Split, predict, update;  $k_e$  and  $k_o$  normalize the energy of the underlying scaling and wavelet functions. (Source: Claypoole and Baraniuk (2000))

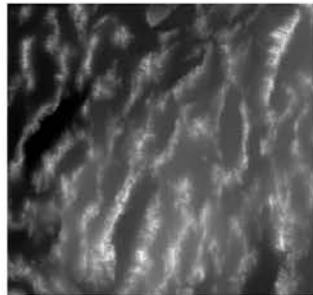


Fig. 3: The GTOPO30 DEM of Great Basin. The elevation values of the terrain (minimum 1005 m and maximum 3651 m) are rescaled to the interval of 0 to 255 (the brightest pixel has the highest elevation). The scale is approximately 1:3,900,00

is a flexible technique that has been used in several different settings, for easy construction and implementation of traditional wavelets and of second generation wavelets, such as spherical wavelets. Lifting consists of the following three basic operations (Fig. 2):

**Step 1**

**Split:** The original data set  $x[n]$  is divided into two disjoint subsets, even indexed points  $x_e[n] = x[2n]$  and odd indexed points  $x_o[n] = x[2n+1]$ .

**Step 2**

**Predict:** The wavelet coefficients  $d[n]$  are generated as the error in predicting  $x_o[n]$  from  $x_e[n]$  using the prediction operator  $P$ :

$$d[n] = x_o[n] - P(x_e[n]) \tag{6}$$

**Step 3**

**Update:** Scaling coefficients  $c[n]$  that represent a coarse approximation to the signal  $x[n]$  are obtained by combining  $x_e[n]$  and  $d[n]$ . This is accomplished by applying an update operator  $U$  to the wavelet coefficients and adding to  $x_e[n]$ :

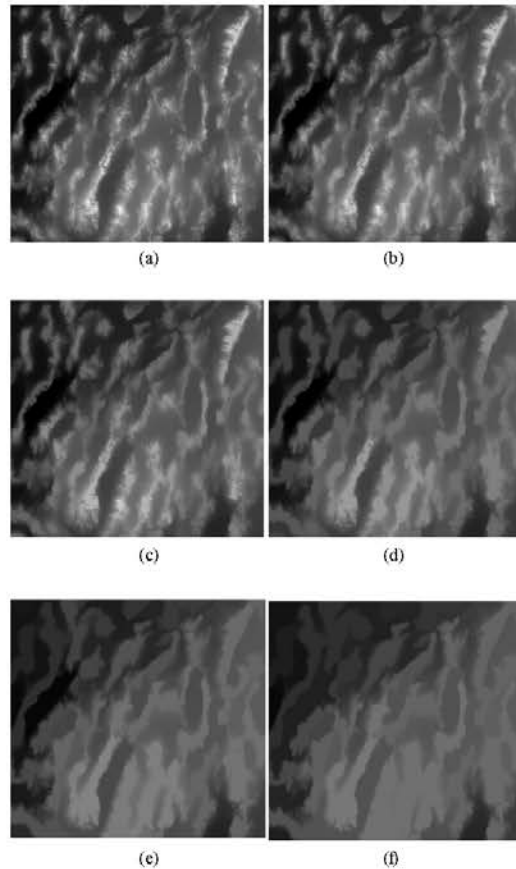


Fig. 4: Multiscale DEMs generated using scales of (a) 1, (b) 3, (c) 5, (d) 10, (e) 15 and (f) 20

$$c[n] = x_e[n] + U \tag{7}$$

These three steps form a lifting stage. Using a DEM as the input, an iteration of the lifting stage on the output  $c[n]$  creates the complete set of multiscale DEMs  $c_j[n]$  and the elevation loss caused by the change of scale  $d_j[n]$ .

The DEM in Fig. 3 shows the area of Great Basin, Nevada, USA. The area is bounded by latitude  $38^\circ 15'$  to  $42^\circ N$  and longitude  $118^\circ 30'$  to  $115^\circ 30' W$ . The DEM was rectified and resampled to 925 m in both  $x$  and  $y$  directions. The DEM is a Global Digital Elevation Model (GTOPO30 DEM) and was downloaded from the USGS GTOPO30 website (<http://edcwww.cr.usgs.gov/landdaac/topo30/topo30.html>). GTOPO30 DEMs are available at a global scale, providing a digital representation of the Earth's surface at a 30 arc-seconds sampling interval. The land data used to derive GTOPO30 DEMs are obtained from digital terrain elevation data (DTED), the 1-degree DEM for USA and the Digital Chart of the World (DCW). The accuracy of GTOPO30 DEMs varies by location according to the source data. The DTED and the 1-degree

dataset have a vertical accuracy of  $\pm 30$  m while the absolute accuracy of the DCW vector dataset is  $\pm 2000$  m horizontal error and  $\pm 650$  vertical error (Miliareis and Argialas, 2002). Tensional forces on the terrain's crust and thins by normal faulting have caused the formation an array of tipped mountain blocks that are separated from broad plain basins, producing a basin-and-range physiography (Howell, 1995).

Multiscale DEMs of the Great Basin region are generated by implementing the lifting scheme on the DEM of Great Basin using scales of 1 to 20. As shown in Fig. 4, as the scale increases, the merge of small regions into the surrounding grey level regions increases, causing removal of fine detail in the DEM.

**APPLICATION OF OPENING BY RECONSTRUCTION TO CHARACTERIZE THE SIZEDISTRIBUTION OF MOUNTAINSEXTRACTED FROM MULTISCALE DEMS**

The mountains extraction algorithm proposed in Dinesh (2006) is implemented on the generated multiscale DEMs. As shown in Fig. 5, the merge of small regions into the surrounding grey level regions increases and the removal of fine detail cause a reduction in the area of the extracted mountains.

The size distribution of the extracted mountains is characterized by performing opening by reconstruction

iteratively on the extracted mountains using square kernels of increasing size. In each iteration, opening removes mountain objects that are unable to completely cover the kernel, while modifying the shape of the remaining mountain objects. The reconstruction step returns the original shape of the remaining mountain objects. The number of mountain objects remaining  $N$  and the total area of the remaining mountain objects  $S$  are computed.

Log-log plots of  $N$  against  $S$  are drawn for the mountains extracted from the generated multiscale DEMs (Fig. 6). For each plot, the slope and y-intercept is computed. In each of the plots, a power law relationship is observed between the two parameters. In general, these power laws take the following form

$$N = c * S^D \tag{8}$$

This power law arises as a consequence of the fractal properties of the size distribution of the extracted mountain objects. In Eq. 7,  $c$  is a constant of proportionality, while  $D$  is the fractal dimension of the size distribution of the extracted mountain objects  $D$ , which indicates the variability of the size distribution of the extracted mountain objects; a higher value of  $D$  indicates a more varied distribution, while a lower value of  $D$  indicates a more even distribution.

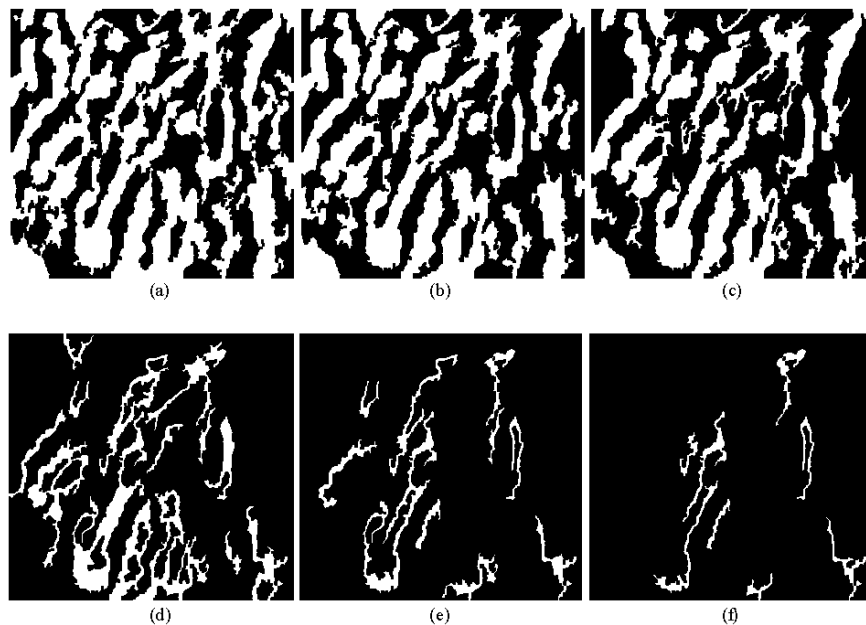


Fig. 5: The mountains extracted from the corresponding multiscale DEMs in Fig. 4. The white pixels represent mountain regions, while the black pixels represent non-mountain regions

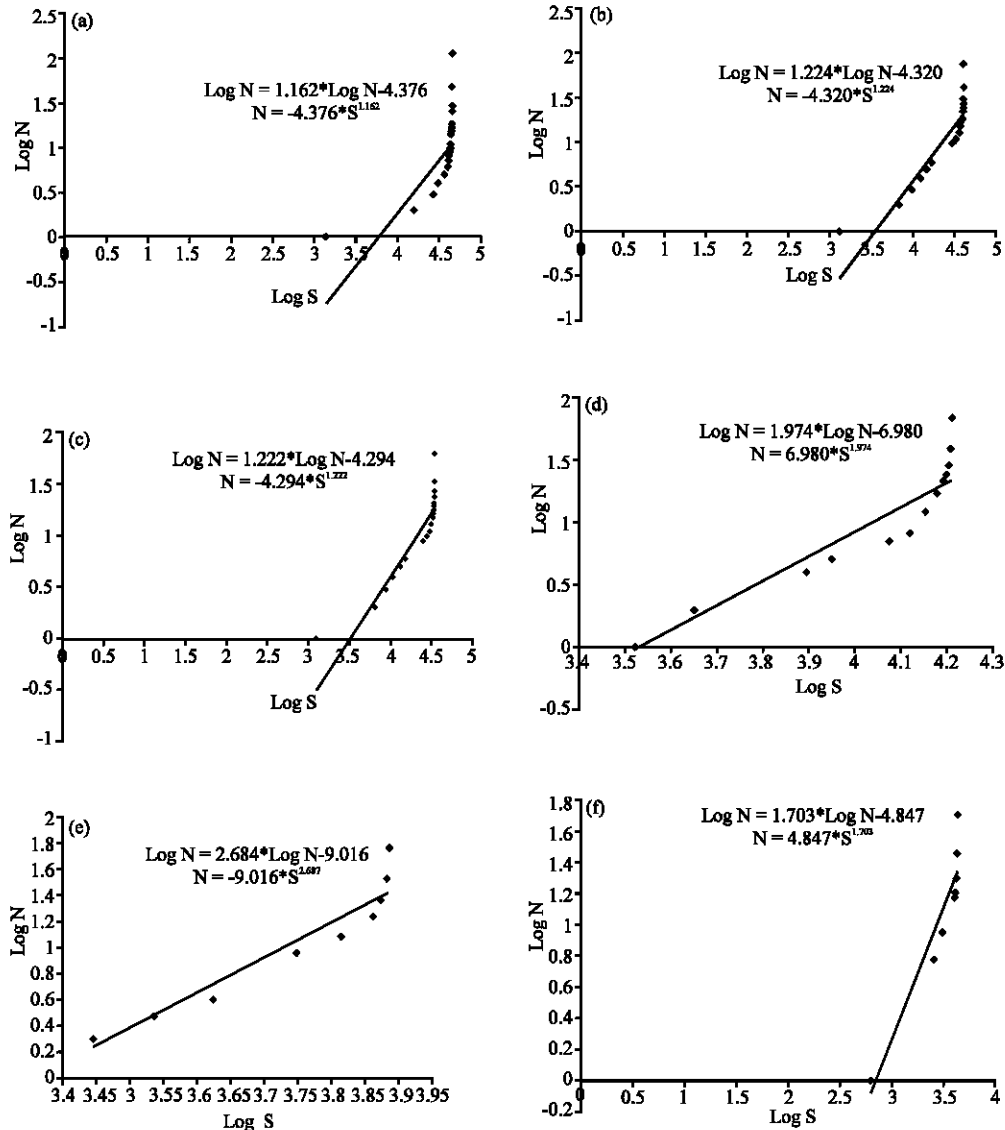


Fig. 6: Log-log plots of the No. of remaining mountain objects N against the total area of remaining mountain objects S

**CONCLUSION**

In this study, the characterization of the size distribution of mountains extracted from multiscale DEMs was performed by performing opening reconstruction iteratively on the extracted mountains. A power law relationship is observed between the number and total area of mountain objects remaining. This power law arises as a consequence of the fractal properties of the size distribution of the extracted mountains. More experiments are being carried out to further quantify the fractal properties of the size distribution of mountains extracted from multiscale DEMs.

**REFERENCES**

Bates, R.L. and J.A. Jackson, 1987. Glossary of geology. American Geological Institute, Alexandria, Virginia.

Claypoole, R.L. and R.G. Baraniuk, 2000. A Multiresolution Wedgelet Transform for Image Processing. In: Wavelet Applications in Signal and Image Processing VIII, Unser, M.A., A. Aldroubi and A.F. Laine (Eds.) Vol. 4119 of SPIE Proceedings, pp: 253-262.

Dinesh, S., 2006. Extraction of mountains from digital elevation models using mathematical morphology. GIS Malaysia, 1: 16-19.

- Graff, L.H. and E.L. Usery, 1993. Automated classification of generic terrain features in digital elevation models. *Photogrammetric Eng. Remote Sens.*, 59: 1409-1417.
- Howell, D., 1995. *Principles of Terrain Analysis: New Applications for Global Tectonics*. Chapman and Hall, London.
- Matheron, G., 1975. *Random Sets and Integral Geometry*. Wiley, New York.
- Miliareisis, G.C. and D.P. Argialas, 1999. Segmentation of physiographic features from Global Digital Elevation Model/GTOPO30. *Computers and Geosciences*, 25: 715-728.
- Miliareisis, G.C., 2000. The DEM to mountain transformation of zagros ranges. 5th International Conference on GeoComputation, 23-25 of August 2000, University of Greenwich.
- Miliareisis, G.C. and D.P. Argialas, 2002. Quantitative representation of mountain objects extracted from the Global Digital Elevation Model (GTOPO30). *Int. J. Remote Sens.*, 23: 949-964.
- Serra, J., 1982. *Image Analysis and Mathematical Morphology*. Academic Press, London.
- Soille, P., 2003. *Morphological image analysis: Principles and applications*. Springer Verlag, Berlin.
- Soille, P. and M.M. Ansoult, 1990. Automated basin delineation from digital elevation models using mathematical morphology. *Signal Processing*, 20: 171-182.
- Sweldens, W., 1996. The lifting scheme: A custom-design construction of biorthogonal wavelets. *Applied Comput. Harmon. Anal.*, 3: 186-200.
- Sweldens, W., 1997. The lifting scheme: A construction of second generation wavelets. *J. Math. Anal.*, 29: 511-546.
- Tate, N. and J. Wood, 2001. Fractals and Scale Dependencies in Topography. In: *Modelling Scale in Geographical Information Science*. Tate, N. and P. Atkinson (Eds.), Wiley, Chichester, pp: 35-51.
- Vincent, L., 1993. Morphological reconstruction in image analysis: Applications and efficient algorithms. *IEEE Trans. Image Process.*, 2: 176-201.
- Wood, J., 1996a. Scale-Based Characterization of Digital Elevation Models. In: *Innovation in GIS 3*. Parker, D. (Ed.), Taylor and Francis, London, pp: 163-175.
- Wood, J., 1996b. The geomorphological characterization of digital elevation models, Ph.D Thesis, University of Leicester, Leicester.